ORIGINAL PAPER

Structural and optoelectrical properties of nanocrystalline Gd-doped CdO films prepared by sol gel method

A. A. Dakhel · A. Y. Ali-Mohamed

Abstract Gd-doped CdO thin films with various Gd concentrations have been prepared on glass and Si wafer substrates using sol gel technique. The films were characterised by X-ray fluorescence (XRF), X-ray diffraction (XRD), optical absorption spectroscopy, and dc-electrical measurements. XRF method was used to determine the %Gd content in the films while XRD was used to study the influence of Gd doping on the detailed crystalline structure. Experimental data indicate that Gd^{3+} doping with level of less than 2.4% slightly enlarge the CdO crystalline unit cell. The bandgap (E_g) of Gd-doped CdO suffers narrowing by about 13% due to a small (0.2%) doping level but with %Gd doping level larger than 2.4%, E_g becomes wider than that of undoped CdO. The electrical behaviours of the Gd-doped CdO films show that they are degenerate semiconductors. The 2% Gd-doped CdO film shows increase in its mobility by about 92%, conductivity by 320%, and carrier concentration by 127%, relative to undoped CdO film. From transparent-conducting-oxide point of view, the Gd doping of CdO by sol gel method is not effective. Finally, the absorption in the NIR spectral region was investigated to be due to the free electrons.

Keywords Sol gel method ·
Cadmium-gadolinium oxide · Gd-doped CdO ·
Degenerate semiconductors · Rare earth oxides ·
TCO

A. A. Dakhel (✉)
Department of Physics, College of Science, University
of Bahrain, P.O. Box 32038, Bahrain, Kingdom of Bahrain
e-mail: adakhil@sci.uob.bh

A. Y. Ali-Mohamed
Department of Chemistry, College of Science, University
of Bahrain, P.O. Box 32038, Bahrain, Kingdom of Bahrain

1 Introduction

Cadmium oxide CdO semiconductor has attracted considerable attention in recent years owing to its electrical and optical properties. It has many applications in field of optoelectronics like transparent conducting oxide (TCO), solar cells, flat panel display, optical communications, photo-transistors, as well as other type of applications like gas sensors, low-emissive windows, thin-film resistors… etc [1–5]. The nonstoichiometric CdO thin films has unique physical properties such as n-type degenerate semiconducting properties with relatively high electrical conductivity (10^2–10^4 S/cm) mainly due to oxygen vacancies and Cd interstitials, and transparency in visible and NIR spectral regions with a direct bandgap of 2.2–2.7 eV [1, 6–10]. The optical and electrical properties of CdO can be modified by doping with different metallic ions like In, Sn, Al, Sc, Y, Tl, etc, which improves its TCO properties [1, 5, 11–16]. Moreover, doping of CdO with magnetic ions like Fe [17] or rare-earth 4f-ions like Sm and Dy [18, 19] might combine some magnetic properties with its optoelectronic properties for different applications. In general, it was observed that when the dopant ions have radius smaller than that of Cd^{2+} then the conductivity of the doped CdO increases and the lattice unit cell compresses. CdO crystallises in a cubic structure of Fm3m space group of 6-coordination [20]. The 6-coordination ionic radius of Cd^{2+} is 0.095 nm. The ionic radius of Gd^{3+} is 0.0938 nm when it occupies a 6-coordination position like lattice positions in CdO structure [21], but the standard ionic radius of Gd^{3+} is 0.1078 nm [22], which is slightly larger than that of 6-coordination Cd^{2+}.

Doping of CdO with different ions can be realised by several well-known methods and the sol-gel method is one of them. The present work reports the electrical and optical

properties of Gd-doped CdO prepared by sol-gel method with different doping levels. It must be mentioned that, the doping of CdO with Gd ions by sol gel method, to our best knowledge, is absent from the literature.

2 Experimental

Undoped and Gadolinium-doped CdO films were prepared on glass substrates by sol-gel method using a spin-coating technique. Methanol (CH_3OH), cadmium acetate dehydrate ($Cd(CH_3COO)_2$), glycerol ($C_3H_5(OH)_3$), triethylamine ($N(CH_2CH_3)_3$), and gadolinium acetylacetonate [$Gd(CH_3 COCHCOCH_3)_3 \cdot xH_2O$] or $Gd(acac)_3$ have been used as starting precursors of analytical grade. The CdO precursor is prepared from two solutions by the following procedure. The first solution was made from total dissolving of 2.0 g of cadmium acetate dehydrate in 3.5 ml of methanol with constant magnetic stirring. Then, by slowly addition of 0.11 ml of glycerol under constant stirring, a transparent solution will be obtained. The second solution has been obtained separately dissolving 0.52 ml of triethylamine in 3.5 ml of methanol. This solution was then slowly added to the first one. All the procedure was done at room temperature without water being involved. The resulting solution was completely transparent and only turbidity was observed 12 days after preparation. For doping of Gd, an appropriate quantity of Gd acetylacetonate was added to the first solution. The final solution that contains Gd acetylacetonate was slightly yellow.

The glass slide substrates were cleaned subsequently with acetone and methanol each for five min, deionised water, dilute HCl solution for 10 min, and finally rinsed with deionised water and dried under nitrogen gas flow. The coating solution was dropped on the glass slide and then rotated at 2,000 rpm for 1 min using a spin coater. After the spin coating, the film was dried in oven prepared at 200 °C for 10 min in a furnace in order to evaporate the solvent. The temperature was chosen in order to obtain final dense and good adherence to the substrate film. This procedure was repeated five times before the film was finally inserted inside the furnace prepared at 400 °C for 1 h annealing in air followed by slowly cooling with the furnace. The deposited film thickness was measured after annealing by an MP100-M spectrometer (Mission Peak Optics Inc., USA) to be in the range 0.15–0.25 μm. The structure of the prepared films was studied by the X-ray diffraction (XRD) method using a Philips PW 1710 θ–2θ system with a Cu K_α radiation (0.15406 nm) and a step of 0.02^o. The energy dispersion X-ray fluorescence (EDX) method was used to determine the relative weight ratio Gd to Cd (r) in the studied films. The spectral optical transmittance T(λ) was measured at normal incidence in

UV-VIS-NIR spectral region (300–3,000 nm) with a Shimadzu UV-3600 double beam spectrophotometer. The electrical measurements were carried out with a standard Van-der-Pauw method with aluminium dot contacts in a magnetic field of about 1 T and using a Keithley 195A digital multimeter and a Keithley 225 current source.

3 Results and discussion

3.1 Characterisation by X-rays

The energy-dispersive X-ray fluorescence (EDX) spectrums of the prepared undoped and Gd-doped CdO film are presented in Fig. 1. The spectrum shows the Cd L-spectrum (3.13–3.53 keV) and Gd L_α signal (6.05 keV) with the exciting Cu K_α signal. The ratio of integral intensity of Gd L_α-signal, I_{Gd} to that of Cd L-spectrum, I_{Cd} or (I_{Gd}/I_{Cd}) was used to determine the fractional weight ratio of Gd to Cd in a film sample. For that purpose, the known method of micro radiographic analysis was used [23]. The reference samples were pure Gd_2O_3 and CdO thin films. The result was 0.2, 0.7, 2.0, 2.4, and 3.2% (wt).

Figure 2a shows the X-ray diffraction (XRD) patterns of the prepared undoped and Gd-doped CdO films. The patterns reveal that all the investigated films are polycrystalline with the cubic Fm3m CdO structure [20]. The usually energetically favourable (111) preferred orientation growth of CdO films, prepared by different techniques [24–27], is studied here through the texture coefficient (TC). It is defined [28] as, $TC(hkl) = [nI_r(hkl)/I_{std}(hkl)]/[\sum_{k=1}^{n} I_r^k(hkl)/I_{std}^k(hkl)]$, where $I_r(hkl)$ is the relative intensity of reflection from a given (hkl) plane, $I_{stn}(hkl)$ is the relative intensity of the reflection from the same plane as indicated
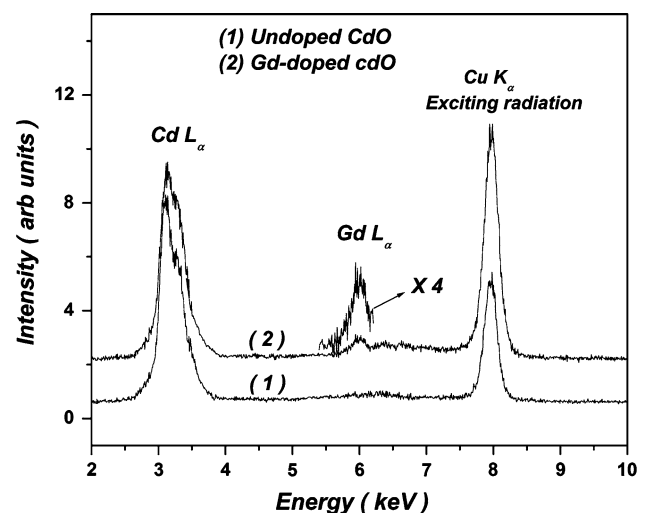

Fig. 1 X-ray fluorescence of undoped and Gd-doped CdO films grown on Si substrate. The exciting radiation was Cu K_α

in a standard sample (ref. [20]), and n is the total number of reflections observed, which are four: 111, 200, 220, and 311. The calculated values of TC are given in Table 1. In general the values of TC shows that all the films are close to be pure polycrystalline, for which TC = 1. The mean X-ray grain size (GS) was estimated by using Scherrer's relation [29]. The results reveal that doping with Gd did not show any appreciable effect on the GS, which was 22–23 nm i.e. the samples were nano crystalline films. It would be expected that a slight shift in reflections from Gd-doped CdO relative to the corresponding reflections from undoped CdO film. This must happen due to a slight difference in ionic sizes of the dopant Gd^{3+} ions and the medium Cd^{2+} ions. Therefore, such doping must creates a structural strain that causes the angular distance between (111) and (200) reflections [$\Delta(2\theta^{\circ})$] of Gd-doped CdO films to be changed relative to that of undoped CdO. The angular distance [$\Delta(2\theta^{\circ})$] is inversely proportional to the lattice parameter (a). Table 1 shows the difference, $\Delta(2\theta^{\circ}) = 2(\theta_{(111)} - \theta_{(200)})$ and volume of the unit cell (v_{unit}) for undoped and Gd-doped CdO. (It was used the followings quite good approximation: $\sin^{-1}(\lambda/a) = (\lambda/a) + (\lambda/a)^{3}/6$ and $\sin^{-1}(3^{1/2}\ \lambda/2a) = (3^{1/2}\ \lambda/2a) + (3^{1/2}\ \lambda/2a)^{3}/6$ for $\lambda/a < 1$. The obtained third order algebraic equation was solved by Cardano's method). One can observe a canonical dependence of v_{unit} on %Gd doping level (Fig. 2b) such that the v_{unit} increases by the doping with Gd^{3+} of ionic standard radius (0.1078 nm) larger than that of Cd^{2+}. This increasing becomes the largest with 2.4%Gd referring to the largest possibility of Gd ion doping by using the present sol gel method.

3.2 DC-electrical properties

The room temperature electrical resistivity (ρ), mobility (μ_{el}), and carrier concentration (N_{el}) were measured by a standard Van-der-Pauw method and the results are presented in Table 2 and Fig. 3. The main source of experimental error is being due to the sample size and circular-aluminium contact spot size, which was estimated to be about 5%. The electrical measurements show that all Gd-doped CdO films are n-type semiconductors. Compared with previous investigations [1, 30–35], the conductivity of undoped CdO is smaller than previously mentioned values ($\sigma \sim 10^{3}$–10^{4} S/cm) due to different procedure of preparation. In addition, the measured carrier concentration in the present work is larger than the known values ($\sim 10^{19}$–10^{20} cm^{-3}) for undoped CdO. This high carrier concentration contributed by shallow donors resulting from nonstoichiometry. The high carrier concentration of undoped CdO found in the present work strongly reduces the carrier mobility. The present results show that CdO doping with Gd ions changes all its electrical parameters in a
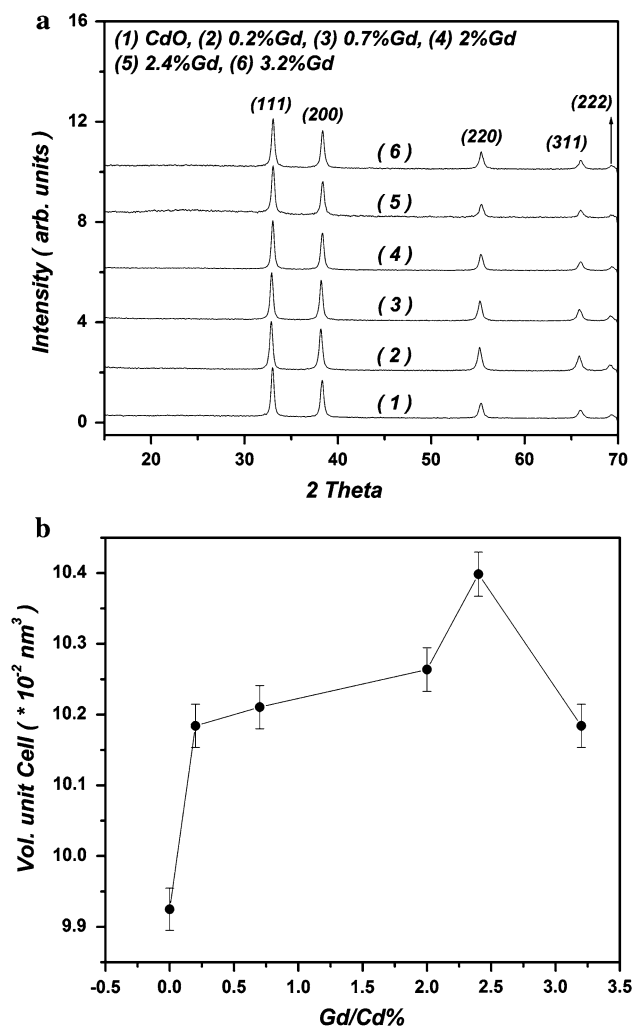
Fig. 2 **a** X-ray diffraction patterns from undoped and Gd-doped CdO films prepared at different Gd% dopant levels. The used radiation was Cu K$_{\alpha}$- line. **b** Dependence of the volume of unit cell of Gd-doped CdO on the Gd% doping level with estimated *error bars*

Table 1 The Bragg angle difference [$\Delta(2\theta^{\circ})$], the volume of unit cell (v_{unit}), and the texture coefficient [TC(111)] for the prepared undoped and Gd-doped CdO films on glass substrates

Sample	$\Delta(2\theta^{\circ})$	v_{unit} (*10^{-2} nm^{3})	TC(111)
CdOsolgel	5.355	9.925	1.30
0.2%Gd	5.305	10.184	1.00
0.7%Gd	5.300	10.211	1.25
2.0%Gd	5.290	10.264	1.06
2.4%Gd	5.265	10.398	1.38
3.2%Gd	5.305	10.184	1.22

complicated manner, as shown in Fig. 3. The carrier concentration decreases at the low Gd% loading. It reaches some lower value at 0.7%Gd, then it suddenly increases by about 4.6 times at 2.0%Gd, where the resistivity reaches its lowest value. The mobility, as resultant of the resistivity
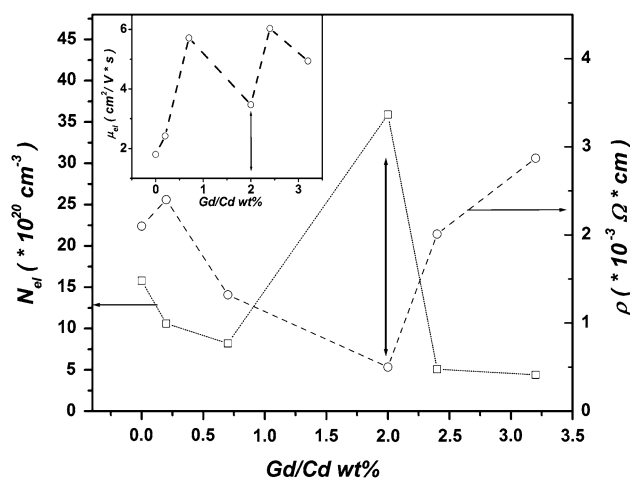
and carrier concentration $\mu_{el} = (e\rho N_{el})^{-1}$, gets its higher value for 0.7%Gd film, then strongly reduces with 2%Gd film accompanied by a strong increase of carrier concentration. Identical behaviour of variation of μ_{el} and TC with the %Gd doping level was observed. This means that the grain boundary scattering plays an important role for the scattering in addition to carrier concentration effect. The process of doping with Gd ions includes many routes: the replacements of Cd^{2+} ions by Gd^{3+} ions, the insertion of Gd^{3+} ions in interstitials, and the dispersing on CdO nanoparticles in form of small Gd-oxide cluster (i.e. grain boundary (GB) accumulation effect). The resultant of all these processes controls the data of Fig. 3. The GB accumulation effect at concentrations larger than 2.4% appears predominately over the other two mechanisms. From TCO point of view, Gd doping of less than 2.0% can be used to increase the conductivity and mobility relative to undoped sol-gel CdO. However, this improvement cannot emulate those films prepared by other methods of preparation. In a summary, the present work proves that low doping with Gd improves the dc-conduction parameters of CdO, so that the 2.0% Gd-doped CdO film shows an increase in its mobility by about 2 times, conductivity by 4 times, and carrier concentration by 2.3 times in comparison with undoped CdO film.

3.3 Optoelectronic properties

The spectral optical absorption measurements are used to study the optical properties of the prepared undoped and Gd-doped CdO films grown on corning glass substrates. The experimentally corrected normal spectral absorbance $A(\lambda)$ in the UV-VIS-NIR region (300–3,000 nm) are presented in Fig. 4 as absorption coefficient $\alpha(\lambda)$, where $\alpha(\lambda) = A(\lambda)/d$ and d is the film thickness. Any special absorption peak or feature in the wavelength range studied that is related to 4f electrons (like 4f–5d transition) was not observed. The spectra show that the minima of the spectral absorbance for all the investigated films are being in the NIR region. In addition, at NIR region for $\lambda > 2,500$ nm, the absorption curves show a clear growth with λ, due to
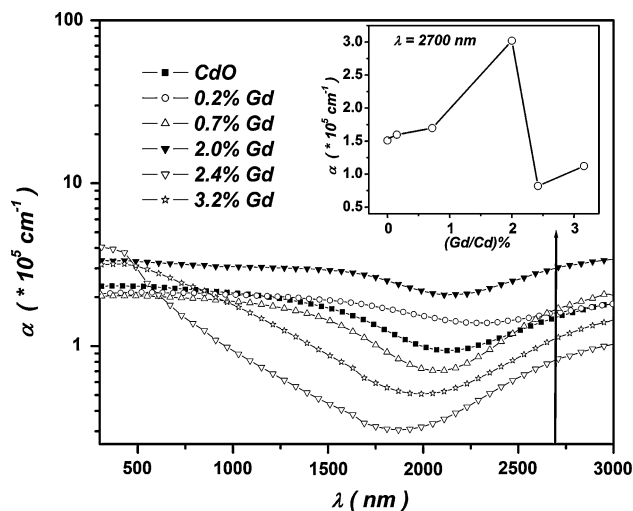

Fig. 3 Variation of resistivity (ρ), carrier concentration (N_{el}), and mobility (μ_{el}) (*inset*) of undoped and Gd-doped CdO films prepared on glass substrates with Gd% dopant level

the high density of free electrons. The inset of Fig. 4 demonstrating the dependence of α at 2,700 nm (NIR) on Gd% content is totally agree with the dependence of N_{el} on Gd% content (Fig. 3). This agreement refers to the fact that both dependences are related to the same conduction electrons. This fact was known previously as that the absorption in the NIR spectral region is mainly caused by the free carriers according to classical Drude theory.

The optical direct bandgap E_g is evaluated with the well-known relationship [36, 37]:
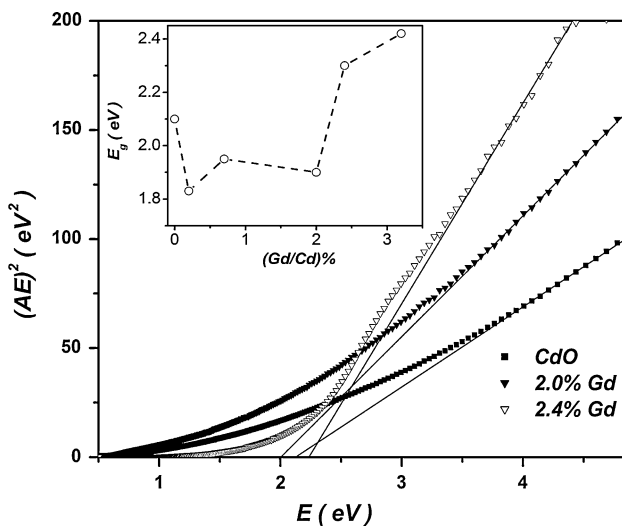
$$AE = B_{Op}(E - E_g)^m \qquad (1)$$

where A is the film absorbance, E is the energy, B_{Op} is a constant of the film and the exponent m is equal to 0.5 or 2

Table 2 Summary of the measured electrical parameters [resistivity (ρ), mobility (μ_{el}), and carrier concentration (N_{el})], and bandgap (E_g) for undoped and Gd-doped CdO films on glass substrates

Sample	ρ ($\times 10^{-3}\Omega^*cm$)	μ_{el} (cm^2/V^*s)	N_{el} ($10^{20}\ cm^{-3}$)	E_g (eV)
CdOsolgel	2.10	1.80	15.8	2.1
0.2%Gd	2.40	2.42	10.6	1.83
0.7%Gd	1.32	5.71	8.2	1.95
2.0%Gd	0.50	3.47	35.9	1.9
2.4%Gd	2.01	6.03	5.1	2.3
3.2%Gd	2.87	4.94	4.4	2.4

Fig. 4 Spectral normal absorption coefficient $\alpha(\lambda)$ in the UV-VIS-NIR spectral regions for undoped and Gd-doped CdO films prepared on glass substrates at different Gd% dopant levels. The *inset* shows the dependence of α at 2,700 nm (NIR) on the Gd% dopant level

for direct and indirect transitions, respectively. Thus, the extrapolation of the plot of $(AE)^2$ versus E for any film gives the value of direct bandgap. Figure 5 demonstrates the bandgap plot for only three concentrations for better clarity. The inset of Fig. 5 shows the variation of E_g with the %Gd doping level. With increasing the %Gd doping level, the bandgap decreases till some lowest value before increasing getting values larger than that of the undoped CdO.

The obtained bandgaps for undoped and Gd-doped CdO films are given in Table 2. For undoped CdO, the bandgap obtained is in the range (2.2–2.6 eV) that is known for undoped CdO films prepared by different techniques [1, 38, 39]. It is obvious that the bandgaps of Gd-doped CdO films with doping levels up to 2% are narrower than that of undoped CdO film. For example, doping of CdO with 0.2%Gd narrows the bandgap by about 13%. The bandgap narrowing can be explained by the joining of impurity levels in the bandgap with the bottom of the conduction band. However, to analyse such behaviour, we combine several phenomenological models in order to relate the bandgap variations to the carrier concentration. The *BGW* is given by the following relation [12, 13]: $\Delta E_g^{BM} = S_{BGW} N_{el}^{2/3}$, where $S_{BGW} = (\hbar^2/2\gamma m_e)(3\pi^2)^{2/3}$, $\hbar$ is the Plank's constant and $\gamma = m_{vc}^*/m_e$ is the ratio for of reduced effective mass to free-electron mass, which is equal to 0.274 for undoped *CdO* [38–40]; thus $S_{BGW}^{th} = 1.348 \times 10^{-18} \text{eV} * \text{m}^2$. The *BGN* consists of two parts. The first part arises due to the electron-impurity interaction and is given by the following relation [40, 41]: $\Delta E_{bt} = S_{BGN}^{(1)} N_{el}^{2/3}$, where $S_{BGN}^{(1)} = (1/3)S_{BGW} = 4.49 \times 10^{-19} \text{eV} * \text{m}^2$. The

second part of *BGN* results from the Columbic interaction (*C*–int) between the carriers, and is given by [42, 43] $\Delta E_{C-int} = S_{BGN}^{(2)} N_{el}^{1/3}$, where $S_{BGN}^{(2)} = (e/2\pi\varepsilon_0\varepsilon_r)(3/\pi)^{1/3}$, ε_0 is the permittivity of free space, e is the electronic charge, and for the dielectric constant ε_r it is possible to use ε_∞, thus $S_{BGN}^{(2)} = 2.836 \times 10^{-9}/\varepsilon_r$. Therefore, the total *BGN* is $BGN = (S_{BGN}^{(1)} N_{el}^{2/3} + S_{BGN}^{(2)} N_{el}^{1/3})$ and the overall bandgap shift is given by;

$$\begin{aligned}\Delta E_g = E_g - E_{g0} &= BGW - BGN \\ &= S_{BGW} N_{el}^{2/3} - S_{BGN}^{(1)} N_{el}^{2/3} - S_{BGN}^{(2)} N_{el}^{1/3} + C_f \\ &= S_{BGW,BGN} N_{el}^{2/3} - S_{BGN}^{(2)} N_{el}^{1/3} + C_f \end{aligned} \quad (2)$$

where C_f is the fitting parameter and $S_{BGW,BGN} = S_{BGW} - S_{BGN}^{(1)} = 8.98 \times 10^{-19} \text{eV} * \text{m}^2$ In the present work, a good straight line was obtained by considering the plot of $[E_g - S_{BGW,BGN} N_{el}^{2/3}]$ vs. $N_{el}^{1/3}$, as shown in Fig. 6, with $S_{BGN}^{(2)} = 2.5 \times 10^{-9} \text{eV} * \text{m}$. This value is close to the theoretical one [1, 42] $S_{BGN}^{(2)}(th) = 1.107 \times 10^{-9} \text{eV} * \text{m}$; the slight difference might come from the non-parabolic band effects.

4 Conclusions

We report on the structural, optical, and dc-electrical properties of Gd-doped CdO films prepared by sol gel technique. From structural side, Gd doping with level less than 2.4% slightly expands the unit cell due to the inserting of Gd^{3+} ions into the crystalline structure. These Gd^{3+} ions do not occupying the 6-coordination positions of the CdO structure. For doping level more than 2.4%, the Gd ions accumulate on the grain boundaries in form of oxide clusters. From optical side, it was observed that the low

Fig. 5 Calculated (points) spectral optical absorbance $A(\lambda)$ is plotted as $(AE)^2$ versus photon energy (E) for undoped and Gd-doped CdO: 2%Gd, and 2.4%Gd films. The direct bandgap is determined by the shown extrapolation. The *inset* shows the dependence of found bandgap on the Gd% dopant level
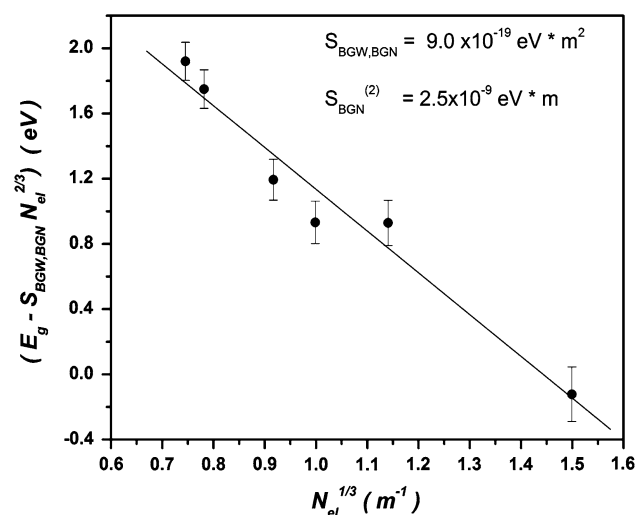

Fig. 6 Dependence of optoelectronic function $(E_g - S_{BGW,BGN} N_{el}^{2/3})$ on the carrier concentration $N_{el}^{1/3}$. The *straight line* represents the best fit in accordance with Eq. 2 with the estimated *error bars*

doping with Gd^{3+} ions (0.2%) shrinks the bandgap of the host CdO by about 13% but with %Gd doping level larger than 2%, E_g becomes wider than that of undoped CdO. The electrical behaviours of the Gd-doped CdO films show that they are degenerate semiconductors. The 2% Gd-doped CdO film shows an increase in its mobility by about 92%, conductivity by 320%, and carrier concentration by 127%, in comparison with undoped CdO film. However, this improvement cannot emulate those films prepared by other methods.

References

1. Zhao Z, Morel DL, Ferekides CS (2002) Thin Solid Films 413:203
2. Su LM, Grote N, Schmitt F (1984) Electron Lett 20:716
3. Gomez Daza O, Arias-Carbajal Readigos A, Campos J, Nair MTS, Nair PK (2001) Mod Phys Lett B 17:609
4. Lewis BJ, Paine DC (2000) Mater Res Soc Bull 25:22
5. Yan M, Lane M, Kannewurf CR, Chang RPH (2001) Appl Phys Lett 78:02342
6. Carballeda-Galicia DM, Castanedo-Perez R, Jimenez-Sandoval O, Jimenez-Sandoval S, Torres-Delgado G, Zuniga-Romero CI (2000) Thin Solid Films 371:105
7. Chopra KL, Ranjan Das S (1993) Thin film solar cells. Plenum Press, NY
8. Choi YS, Lee CG, Cho SM (1996) Thin Solid Films 289:0153
9. Kondo R, Okhimura H, Sakai Y (1971) Jpn J Appl Phys 10:1547
10. Coutts TJ, Young DL, Li X, Mulligan WP, Wu X (2000) J Vac Sci Technol A 18:2646
11. Dakhel AA (2008) Phys Stat Sol (a) 205:2704
12. Burstein E (1954) Phys Rev 93:632
13. Moss TS (1954) Proc Phys Soc Lond B67:775
14. Freeman AJ, Poeppelmeier KR, Mason TO, Chang RPH, Marks TJ (2000) Mater Res Soc Bull 25:45
15. Maity R, Chattopadhyay KK (2006) Sol Energy Mater Sol Cells 90:597
16. Shu S, Yang Y, Medvedova JE, Ireland JR, Metz AW, Ni J, Kannewurf CR, Freeman AJ, Tobin TJ (2004) J Am Chem Soc 126:13787
17. Dakhel AA (2010) Thin Solid Films 518:1712
18. Dakhel AA (2009) J Alloys Compd 475:51
19. Dakhel AA (2009) Sol Energy 83:934
20. Powder Diffraction File, Joint committee for powder diffraction studies (JCPDS) file no. 05-0640
21. Shannon RD (1976) Acta Crystallogr A A32:751
22. Forum Chemi Cool, http://www.chemicool.com/elements/gadolinium.html
23. Jaklevic JM, Goulding FS (1978) Energy Dispersion. In: Herglotz HK, Birks LS (eds) X-ray Spectrometry. M. Dekker, NY, p 50
24. Subramanyam TK, Uthanna S, Naidu BS (1998) Mater Lett 35:214
25. Reddy KTR, Sravani C, Miles RW (1998) J Cryst Growth 184/185:1031
26. Phatak G, Lai R (1992) Thin Solid Films 209:240
27. Tanaka K, Kunioka A, Sakai Y (1969) Jpn J Appl Phys 8:681
28. Barrett CS, Massalski TB (1980) Structure of Metals. Oxford, Pergamon, p 204
29. Kaelble EF (ed) (1967) Handbook of X-rays for diffraction, emission, absorption, and microscopy. McGraw-Hill, New York, p 5-17
30. Chu TL, Chu SS (1990) J Electron Mater 19:1003
31. Gurumurugan K, Mangalaraj D, Narayandass SK (1996) J Electron Mater 25:765
32. Varkey AJ, Fort AF (1994) Thin Solid Films 239:211
33. Reddy KTR, Shanthini GM, Johnston D, Miles RW (2003) Thin Solid Films 427:397
34. Li X, Young DL, Moutinho H, Yan Y, Narayanswamy C, Gessert TA, Coutts TJ (2001) Electrochem solid state lett 4:C43
35. Santos-Cruz J, Torres-Delgado G, Castanedo-Perez R, Jimenez-Sandoval S, Jimenez-Sandovl O, Zuniga-Romero CI, Marques Marin J, Zelaya-Angel O (2005) Thin Solid Films 493:83
36. J. Tauc (1969) Optical properties of solids, Edited by F. Abeles. North Holland
37. Davis EA, Mott NF (1970) Philos Mag 22:903
38. Kawamura K, Maekawa K, Yanagi H, Hirano M, Hosono H (2003) Thin Solid Films 445:182
39. Ueda N, Maeda H, Hosono H, Kawazoe H (1998) J Appl Phys 84:6174
40. Hahn D, Jaschhinski O, Wehmann H–H, Schlachetzki A (1995) J Electron Mater 24:1357
41. Bugajski M, Lewandowski W (1985) J Appl Phys 57:521
42. Wolff PA (1962) Phys. Rev. 126:405
43. Camassel J, Auvergne D, Mathieu H (1975) J Appl Phys 46:2683